2015-07-07

Mechanical Property and Biocompatibility of Co-precipitated Nano Hydroxyapatite-Gelatine Composites

Le, HR

10.1007/s40145-015-0155-z
Journal of Advanced Ceramics
Tsinghua University Press

Mechanical Property and Biocompatibility of Co-precipitated Nano Hydroxyapatite-Gelatine Composites

H. R. Le[1*], K. Natesan[2], S. Pranti-Haran[3]

[1]School of Marine Science and Engineering, Plymouth University, United Kingdom
[2]Peninsular Schools of Medicine and Dentistry, Plymouth University, United Kingdom
[3]School of Engineering, Physics and Mathematics, University of Dundee, United Kingdom

*Corresponding Author (H. R. Le): Tel +44 1752 586172, Email: huirong.le@plymouth.ac.uk

Abstract

A uniform and well dispersed nano hydroxyapatite-gelatine composite was obtained by co-precipitation of hydroxyapatite and denatured calf skin collagen. The process allowed much higher concentration of hydroxyapatite to be produced over conventional hydrothermal process to improve the productivity. The effect of gelatine on the morphology, mechanical properties and biocompatibility of hydroxyapatite particles was investigated. Fibroblast cell tests of the consolidated hydroxyapatite-gelatine composite showed that the composite has excellent biocompatibility.

Keywords: Biomaterials, Nanocomposites, Hydroxyapatite, Gelatine, Biocompatibility.

1. INTRODUCTION

An extremely specialized supporting framework of the body protecting the vital organs is bone. Natural bone is a composite material composed of hybrid organic and inorganic constituents. It has a varied arrangement of material structures at many length scales which work in concert to perform diverse mechanical, biological and structural properties. The uninterrupted growth in the age of population has led to continuous conditions which are prone to injury causing severe damage to the individual. While bone is inherently capable of regeneration, complications such as excessive bone loss impede healing, necessitating the use of bone grafts (1). Bone is one of the most frequently implanted tissues in the human body, second only behind blood. Due to advances in biomaterials research, it is now possible to artificially fabricate materials that mimic the structure of natural bone to be used as bone replacement.

Hydroxyapatite (HA) is the primary inorganic substance in natural bones and has been studied extensively for medical applications due to its excellent bioactivity and biocompatibility. However, pure sintered HA has low fracture toughness and low degradation properties which limit its use to only non-stress applications (2, 3). Previous research (4-11) has shown that a composite can be formed that closely resembles the structure of natural bone tissue by combining a mixture of natural macromolecules such as collagen and synthetic hydroxyapatite particles by hydrothermal process. Although the resulting composites have been proven to have good biocompatibility, they suffer from low modulus.

In order to enrich the characteristics of individual components, organic–inorganic composites can be synthesised through a hybridization route to build a harmonious balance between strength and toughness. One technique of achieving this is the sol-gel process which allows the reinforcement of organic polymers within inorganic calcium phosphates producing organic-inorganic hybrids (12). Fabrication route of HA has a strong influence on the crystal morphology. Even with the sol-gel process, different shapes and sizes ranging from nano to micro particles of HA can be produced by altering the reaction rate, pH and temperature along with the presence or absence of surfactants. To be able to control nucleation and crystal morphology many researchers have attempted to use various surfactants and polymers (13-15) and have successfully grown HA crystals with varying morphology.

Natural macromolecules such as gelatine and chitosan are commonly used as a binder in biomedical applications. These polymers have been used as binders for HA particles or HA have been precipitated in their presence using various techniques (16-18). Gelatine being a denatured form of collagen has many attractive properties such as biocompatibility, plasticity and adhesiveness (16, 19). However, there is still a lack of understanding on the effects of these molecules on HA crystal morphology, its mechanical strength and biocompatibility.

The hard tissue of bone is made up of biological apatite which is a non-stoichiometric hydroxyapatite. Natural bone hydroxyapatite has trace amount of several other ions. The precipitation route of HA has a prominent effect on the morphology, shape and size of HA. Even small differences in stoichiometry, crystallinity or morphology are expected to lead to different chemical, biological and physical behaviour of the material (20-22). The previous study by the authors investigated the effect of pH and temperature on the morphology of sol-gel co-precipitated HA (23). XRD analysis confirmed that the material obtained is mainly HA with trace of brushite ($CaHPO_4 \bullet 2H_2O$). Under desirable conditions, a plate-like structure was developed by self-assembly of columnar crystals. This paper is intended to further report on the effect of the addition of gelatine on the morphology and dispersion of HA particles. The biocompatibility of the obtained HA-gelatine composites from this process will also be reported.

2. EXPERIMENTAL METHODS

2.1 Hydroxyapatite and hydroxyapatite-gelatine composite preparation

A diagrammatic representation of the precipitation process developed previously by the authors is shown in the Figure 1. In this method 0.2 mol/litre calcium chloride and 0.12 mol/litre ammonium hydrogen phosphate solutions were dropped simultaneously into a reaction vessel at a controlled rate of about 0.5 litre/hour using valve controlled burettes. The solution was stirred constantly using magnetic stirrer to maintain constant temperature and to facilitate the reaction. The product first appeared as a gel and then milky suspension with more solutions being added. The Ca to P ratio was maintained at 1.67 by using equal volumes of 0.2 mol/litre calcium containing solution and 0.12 mol/litre phosphate containing solution. The effect of temperature and pH on the morphology of hydroxyapatite was reported by the authors in previous work (23).

To fabricate hydroxyapatite-gelatine composites, calf skin collagen (Sigma-Aldrich, Collagen I) was first dissolved in 0.5mol/litre acetic acid at 40°C under continuous stirring. After collagen becoming a uniform gel, the solution was titrated with 0.5 mol/litre sodium hydroxide solution (NaOH) to the desired pH. Hydroxyapatite was precipitated in the presence of the dissolved collagen with a target collagen to HA ratio of 1:10.

The pH value of all the reactions were maintained at 9 to 9.5 using 0.5 mol/litre sodium hydroxide (NaOH) or 0.5 mol/litre acetic acid (CH_3COOH). The former was used when there was a drop in pH during the reaction and the latter was used when the pH was observed to increase. The magnetic stirrer was kept at constant speed of 300-500 rpm for all the reactions. The reaction vessel temperature was kept at nominal 40˚C. Once the reaction was completed, the reaction vessel containing the product was moved into water bath to age at 40˚C for 24 hours.

After aging, a small volume of the aged precipitate was removed and taken for analysis. The suspension was then filtered to remove excessive water and free ions using vacuum assisted filtering system. The composite suspension was poured into the collection beaker with a filter paper. Once the excessive water was removed from the filter, the next step was to rinse the precipitates using deionised water for several times. Atmospheric impurities and other unwanted ions were removed from the composite with fresh deionised water, including chloride (Cl^-), sodium ions (Na^+) and ammonium ions (NH_4^+) etc.

Whilst applying efficient means of filtering the precipitates, only majority of the free water content was removed. As there was water trapped inside the precipitate vacuum filtration was not enough to remove all of the water content. The precipitate paste was placed into a Petri dish and then kept inside an incubator. The incubator was set to a constant temperature of 40 to 60˚C. The weights of the precipitates were taken at regular intervals so the drying process is continued until a constant weight was achieved.

2.2 Sample preparation for mechanical tests

In order to examine the mechanical modulus and strength of the composites, the dried composite precipitates were mixed with DI water so that the liquid to solid ratio was about 1:1. After regular monitoring on the weight of each of the precipitates that were dried in the oven, the precipitates were taken out at water to solid ratio of about 1:2. A number of test blocks with dimensions of 24 x 4 x 2 mm were prepared from each precipitate using a Tufnol

mould with a rectangular slot. For each composite, the weight for one sample piece was calculated and then placed inside the mould. The load was applied using a hydraulic press. The load was gradually increased to 5 kN (equivalent to a pressure of 50 MPa) and held for 1 minute. This would compress the sample, thereby squeezing out the excessive water content that would not have been removed by incubation. After 1 minute dwell, the load was gradually increased to 10 kN (equivalent to a pressure of 100 MPa) and then held for another 1 minute. By this point the composite would have been suitably compressed to produce a strong rectangular solid block. The solid sample was then popped out from the mould.

2.3 Crystallographic and microstructural characterization

The phase constituents of each precipitate were examined using XRD. Certain amount of dried precipitate block was ground into powder and then pressed into flat sample. X-ray powder diffraction patterns were measured on Rigaku D/max2500 X-ray diffractometer with Cu Kα radiation at a scanning speed of 6°/min in range of 10° to 80°. The operating voltage and current of this XRD machine were 40 kV and 200 mA, respectively. The phases of each precipitate were determined by comparing the XRD patterns with JCPDF database.

Scanning electron microscopes (SEM) were used for studying the morphology of the precipitates fabricated. The machine used was Philips XL 30 ESEM (Dundee). The samples were mounted on aluminium stubs. The surface of the stub had carbon adhesives which hold the samples in place. Then these stubs were moved into a sputter coater. The dried blocks were coated with Gold/ Palladium up to 30 nm of thickness in order to dissipate the fast impinging electrons on the specimens during SEM operation.

2.4 Fibroblast cell test

For the biocompatibility tests of the materials to be carried out, the obtained hydroxyapatite-gelatine composite solid blocks were broken into small test beads of about 4mmx4mm.

The test beads were sterilised by soaking them in ethanol for 4 hrs. The samples were then removed using sterile tweezers and placed in sterile beakers. The beakers were heated to 80°C to dry the ethanol soaked samples. Sterile petri dishes were coated with a layer of silicone to encourage cell growth on the samples than the surface of the petri plate. The cell growth media consisted of Fetal Bovine Serum (FBS) and antibiotic-antimycotic (ABAM) solution. FBS medium provided good nutrient to the cells while the ABAM was used to prevent bacterial and fungal infections.

Once the samples were dry they were moved into the cell growth medium. In this process two volumes of bovine serum of same concentration were used. The composite was kept in one of the volume of bovine serum and in the other volume of the bovine serum fibroblasts of rat tendon were cultured. About 15 micro litres of the cultured rat tendon fibroblast was taken and applied onto the composite sample in the Petri dish. The test was performed for 7 days, with nutrient being replenished every 24 hours. The samples were critical point freeze dried with liquid nitrogen and placed in a freeze drier overnight. They were then mounted on stubs and painted in silver paint (Agar Scientific Ltd). These were placed in an incubator at 40^{o}C for 20 minutes followed by gold coating. These samples were subsequently considered stable and were viewed under SEM.

3. RESULTS AND DISCUSSIONS

3.1 Microstructure of hydroxyapatite

The SEM image of the hydroxyapatite crystals obtained at 40˚C / pH 9 by controlled precipitation process is shown in Figure 2. The hydroxyapatite crystals are typical of interlocked plates and scattered nano-particles. The width of the plates is about 2 μm and the thickness about 80 nm according to SEM measurements. It can be seen that HA has developed a distinctive lenticular crystals and subsequent planar assembly during the aging process.

In order to explain this, various factors such as preparation time and aging period should be taken into consideration. This significant difference in the morphology of the crystals could arise as a result of the mixing rate of the precursor solutions as it has a direct impact on the nucleation of HA. Slow mixing of calcium and phosphate precursors in this process results in less nucleation sites and the growth of primary crystals in lenticular form (24).

3.2 Effect of gelatine on the morphology of HA

The morphology of the HA-gelatine composite prepared at 40˚C / pH 9 is shown in Figure 3. It was noted that collagen fibres are not visible even under high resolution SEM. It is believed that the collagen fibres have been denatured into gelatine in acetic acid solution under the temperature applied (25, 26). The morphology of hydroxyapatite particles is different from that of pure hydroxyapatite prepared under the same conditions. The particles in Figure 3 are typical of spherical granules of about 10-100 nm compared to the particles of 80nm to

1000nm shown in Figure 2. This is inferring that the nucleation rate of HA crystals is much higher due to the presence of gelatine molecules in the suspension. This is a result of lower activation energy required in heterogeneous nucleation of hydroxyapatite crystals on the polypeptide structure of gelatine as described in (27). The primary spherical clusters fuse together to form a much more compact and interconnected material with the organic component acting as an adhesive. There is lower probability to form large agglomerates or plate-like structure because the surface energy of the particles is smaller. Thus a uniform and well dispersed nanostructure was obtained.

XRD analysis shown in Figure 4 showed that hydroxyapatite precipitated in the gel has more significant peak widening than that prepared in water. This confirmed that the grain size is smaller in the presence of gelatine molecules due to heterogeneous nucleation as discussed above.

3.3 Mechanical behaviour of hydroxyapatite-gelatine composite

The pressed bar samples were tested using three point bending tests with a 24mm span. The graph in the Figure 5 is the force-displacement curve obtained for a test block of the prepared composite. From the graph it could be seen clearly of the gradual and uniform increase of the applied force in loading. The dimensions of all of the test blocks were measured before the process, in order to determine the fracture strength of the material. The deflection starts from 0.02mm and runs through a distance up to 0.14mm, where the peak load occurs. There are no signs of artefacts or disturbances observed in the graph. The fracture of the test block occurred at maximum load of 7.9 N. Six samples were tested. The average fracture strength of hydroxyapatite-collagen composite is about 15.7 MPa. This is at the lower end of the strength of cortical bones, but higher than cancellous bones (26). It is believed that the collagen molecules might have been denatured and become gelatine during the fabrication process which is responsible for rather modest fracture strength. Nevertheless, the composite exhibits some extensibility after a crack is initiated. This is owing to the stretching of the organic constituencies in the composite.

3.4 Cytocompatibility

The bovine growth medium provides good source of nutrients for the rat tendon fibroblasts to grow. The SEM observations (Figures 6 – 9) showed that many fibroblast cells were clearly visible on all the specimens after 7 days of tests. The cells were large and flat with numerous

pseudopods. They were highly interconnected and healthy growth was observed on all of the samples. These images are clear evidence of cell attachment and proliferation on the surface of the material. It was also noted that the cells could grow on irregular fractal surface of the samples such as ridges and deep cavities (Figures 6 - 8). It is evident that the material is biocompatible and promotes cell attachment and growth. The denaturisation of collagen does not have any negative impact on the cell adhesion to the surface of the composite. Once these fibroblasts start to grow, they tend to stick to the surface of the composite samples. If there was any contamination of the composite sample, which would produce toxic effects on the living tissues, then the entire bovine serum growth media becomes toxic. This would lead to the death of the cells that were introduced into the growth media.

The growth of new extracellular matrix (ECM) during the cell tests was also noted on the SEM image shown in Figure 8. One can see the lighter globules attached to the cells and the surface of the test material. The morphology of these globules is very different from original material. At nearly 12000 times of magnification (Figure 9), it becomes clear that the globules are porous clusters of nano particles and have a diameter of about 3 μm. The morphology of the globules implies that it was a new precipitate when the material was submerged in the cell culture. One possible explanation is that the hydroxyapatite had dissolved gradually in cell culture and new precipitate of nano-crystals had occurred. These new precipitates could attach to the pseudopods developed on the cell surface to form a good attachment. This observation confirms that the HA-gelatine nanocomposite has the potential to regenerate new bone in desirable environment.

4. CONCLUSIONS

An efficient process based on high-concentration sol-gel precipitation was applied to the fabrication of hydroxyapatite and gelatine composites. The productivity was about two orders of magnitude higher than conventional hydrothermal process. In the presence of gelatine in the solution, uniform and well dispersed nano hydroxyapatite particles were obtained due to heterogeneous nucleation. Fibroblast cell tests on the composite showed excellent biocompatibility. Potential applications of the consolidated material include maxillofacial, skeletal bone grafts and scaffolds for bone tissue engineering.

ACKNOWLEDGMENT

The authors want to thank all the technicians at the School of Engineering, Physics and Mathematics at the University of Dundee for their assistance in the manufacture of the mould and testing rig. The authors are also indebted to Dr Kenneth Donnelly and Dr Robert Keatch for constructive discussions and support.

REFERENCES

1. Chao L, Meng B, Erin YT, Mark SKC, Yuchun L, Mahesh C, et al. Advances in Bone Tissue Engineering. 2013.
2. Nilsson M, Wang J-S, Wielanek L, Tanner KE, Lidgren L. Biodegradation and biocompatibility of a calcium sulphate - hydroxyapatite bone substitute. the journal of bone and joint surgery. 2004;86:120-5.
3. Xu HH, Simon CG, Jr. Fast setting calcium phosphate-chitosan scaffold: mechanical properties and biocompatibility. Biomaterials. 2005;26(12):1337-48.
4. Kikuchi M, Itoh S, Ichinose S, Shinomiya K, Tanaka J. Self-organization mechanism in a bone-like hydroxyapatite/collagen nanocomposite synthesized in vitro and its biological reaction in vivo. Biomaterials. 2001;22(13):1705-11.
5. Kikuchi M, Matsumoto HN, Yamada T, Koyama Y, Takakuda K, Tanaka J. Glutaraldehyde cross-linked hydroxyapatite/collagen self-organized nanocomposites. Biomaterials. 2004;25(1):63-9.
6. Kikuchi M, Ikoma T, Itoh S, Matsumoto HN, Koyama Y, Takakuda K, et al. Biomimetic synthesis of bone-like nanocomposites using the self-organization mechanism of hydroxyapatite and collagen. Composites Science and Technology. 2004;64(6):819-25.
7. Zhang W, Liao SS, Cui FZ. Hierarchical Self-Assembly of Nano-Fibrils in Mineralized Collagen. Chemistry of Materials. 2003;15(16):3221-6.
8. Zhai Y, Cui FZ. Recombinant human-like collagen directed growth of hydroxyapatite nanocrystals. Journal of Crystal Growth. 2006;291(1):202-6.
9. Olszta MJ, Cheng X, Jee SS, Kumar R, Kim Y-Y, Kaufman MJ, et al. Bone structure and formation: A new perspective. Materials Science and Engineering: R: Reports. 2007;58(3–5):77-116.
10. Yoon B-H, Kim H-W, Lee S-H, Bae C-J, Koh Y-H, Kong Y-M, et al. Stability and cellular responses to fluorapatite–collagen composites. Biomaterials. 2005;26(16):2957-63.
11. Kim H-W, Kim H-E, Salih V. Stimulation of osteoblast responses to biomimetic nanocomposites of gelatin–hydroxyapatite for tissue engineering scaffolds. Biomaterials. 2005;26(25):5221-30.
12. Costa HS, Mansur AAP, Pereira MM, Mansur HS. Engineered hybrid scaffolds of poly(vinyl alcohol)/bioactive glass for potential bone engineering applications: synthesis, characterization, cytocompatibility, and degradation. J Nanomaterials. 2012;2012:4-.

13. Wang Y, Chen J, Wei K, Zhang S, Wang X. Surfactant-assisted synthesis of hydroxyapatite particles. Materials Letters. 2006;60(27):3227-31.
14. Wang Y, Zhang S, Wei K, Zhao N, Chen J, Wang X. Hydrothermal synthesis of hydroxyapatite nanopowders using cationic surfactant as a template. Materials Letters. 2006;60(12):1484-7.
15. Walsh D, Kingston JL, Heywood BR, Mann S. Influence of monosaccharides and related molecules on the morphology of hydroxyapatite. Journal of Crystal Growth. 1993;133(1–2):1-12.
16. Ji Yin Y, Zhao F, Feng Song X, De Yao K, Lu WW, Chiyan Leong J. Preparation and characterization of hydroxyapatite/chitosan–gelatin network composite. Journal of Applied Polymer Science. 2000;77(13):2929-38.
17. Shou ZJ, Le HR, Qu SY, Rothwell RA, Mackay RE. Fabrication and Mechanical Properties of Chitosan-Montmorillonite Nano-composite. Key Eng Mater. 2012;512-515:1746-50.
18. Yan YJ, Zhang XJ, Mao HH, Huang Y, Ding QQ, Pang XF. Hydroxyapatite/gelatin functionalized graphene oxide composite coatings deposited on TiO2 nanotube by electrochemical deposition for biomedical applications. Appl Surf Sci. 2015;329:76-82.
19. Kim H-W, Knowles JC, Kim H-E. Hydroxyapatite and gelatin composite foams processed via novel freeze-drying and crosslinking for use as temporary hard tissue scaffolds. Journal of Biomedical Materials Research Part A. 2005;72A(2):136-45.
20. Tadic D, Peters F, Epple M. Continuous synthesis of amorphous carbonated apatites. Biomaterials. 2002;23(12):2553-9.
21. Huang Y, Zhang XJ, Mao HH, Li TT, Zhao RL, Yan YJ, et al. Osteoblastic cell responses and antibacterial efficacy of Cu/Zn co-substituted hydroxyapatite coatings on pure titanium using electrodeposition method. Rsc Adv. 2015;5(22):17076-86.
22. Huang Y, Yan YJ, Pang XF, Ding QQ, Han SG. Bioactivity and corrosion properties of gelatin-containing and strontium-doped calcium phosphate composite coating. Appl Surf Sci. 2013;282:583-9.
23. Le HR, Chen KY, Wang CA. Effect of pH and temperature on the morphology and phases of co-precipitated hydroxyapatite. J Sol-Gel Sci Technol. 2012;61(3):592-9.
24. Koutsopoulos S. Synthesis and characterization of hydroxyapatite crystals: A review study on the analytical methods. Journal of Biomedical Materials Research. 2002;62(4):600-12.
25. Manickavasagam B, inventorextraction of Gelatine. USA2008.
26. Meyers MA, Chen P-Y, Lin AY-M, Seki Y. Biological materials: Structure and mechanical properties. Progress in Materials Science. 2008;53(1):1-206.
27. Takeuchi A, Ohtsuki C, Miyazaki T, Kamitakahara M, Ogata S, Yamazaki M, et al. Heterogeneous nucleation of hydroxyapatite on protein: structural effect of silk sericin. J Roy Soc Interface. 2005;2(4):373-8.

Figures captions:

Figure 1 Co-precipitation of hydroxyapatite-gelatine composite

Figure 2 Closer view of HA crystals prepared at 40˚C / pH 9 by slow precipitation

Figure 3 Morphology of HA-gelatine composite.

Figure 4 XRD Graph of HA (a) deposited with no gelatine, (b) deposited with gelatine

Figure 5 The force-displacement curve of three point bending test of 10% collagen composite

Figure 6 Cell attachments to curved composite surface of HA-gelatine composite

Figure 7 Cell growth on surface ridges of HA-gelatine composite.

Figure 8 Cell growth into surface cavities of HA-gelatine composite

Figure 9 Material regeneration during fibroblast cell tests

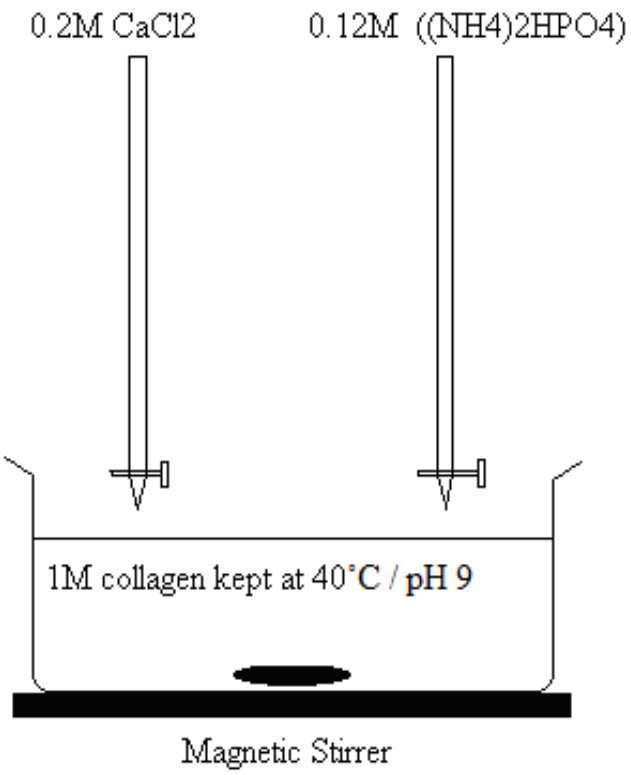

Figure 1 Co-precipitation of hydroxyapatite-gelatine composite

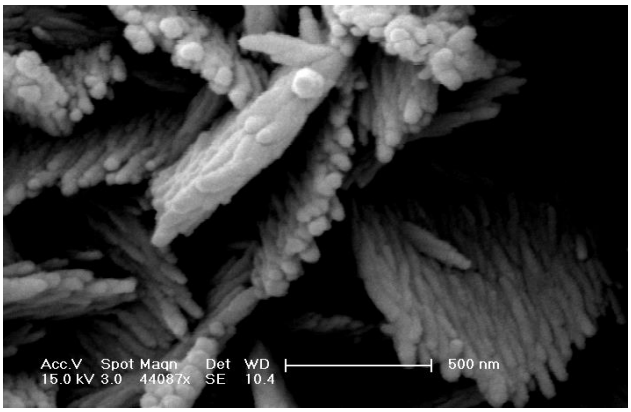

Figure 2 Closer view of HA crystals prepared at 40˚C / pH 9 by slow precipitation

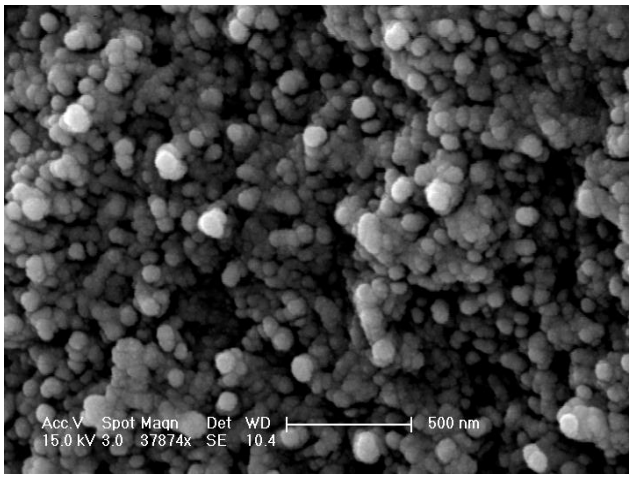

Figure 3 Morphology of HA-gelatine composite.

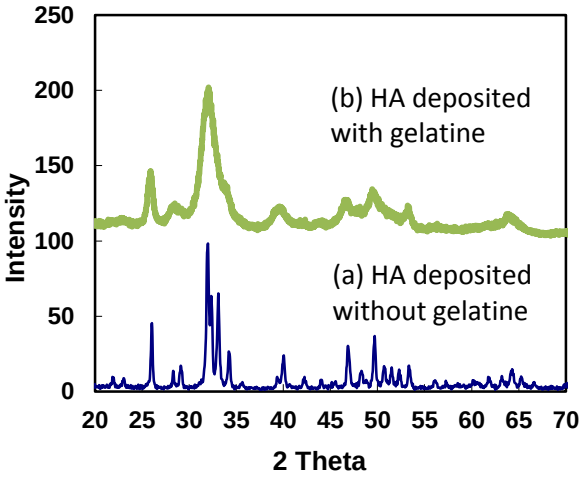

Figure 4 XRD Graph of HA (a) deposited with no gelatine, (b) deposited with gelatine

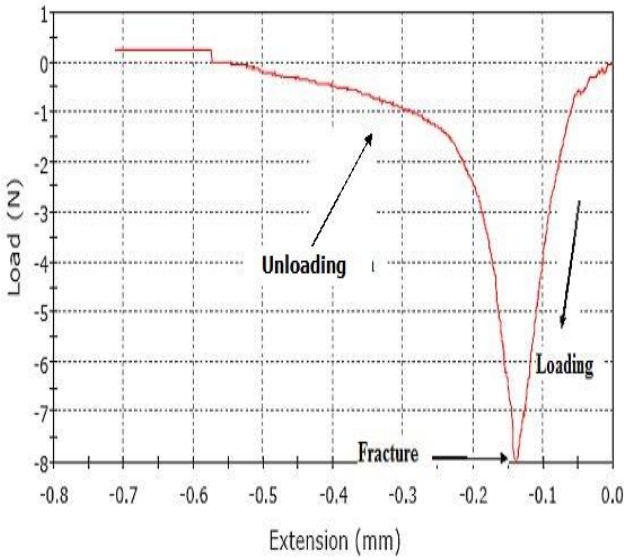

Figure 5 The force-displacement curve of three point bending test of 10% collagen composite

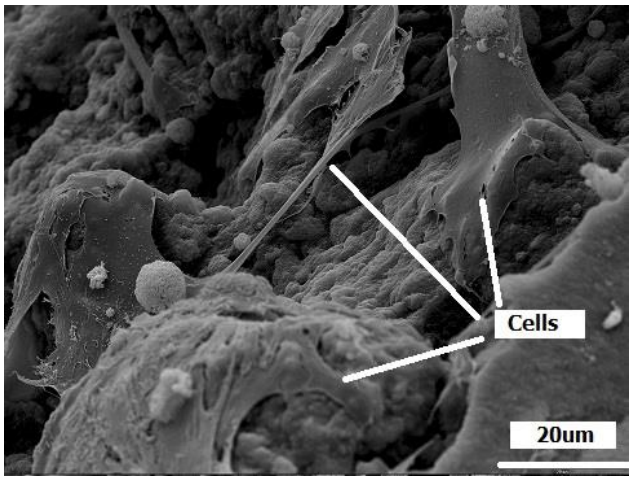

Figure 6 Cell attachments to curved composite surface of HA-gelatine composite

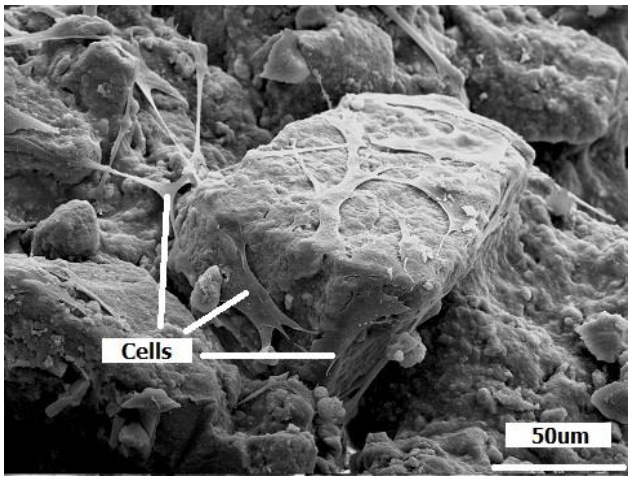

Figure 7 Cell growth on surface ridges of HA-gelatine composite.

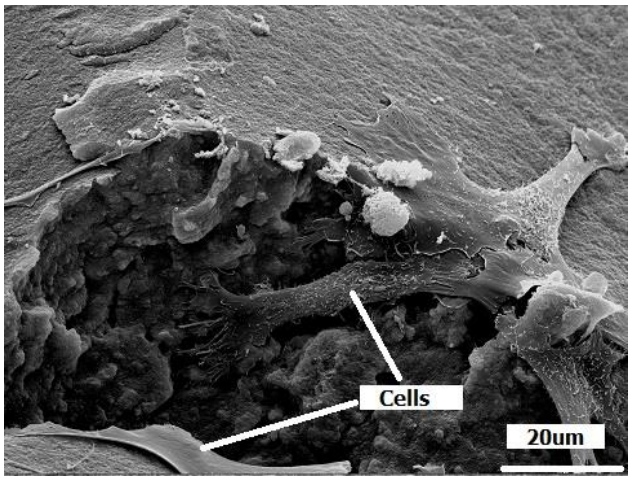

Figure 8 Cell growth into surface cavities of HA-gelatine composite

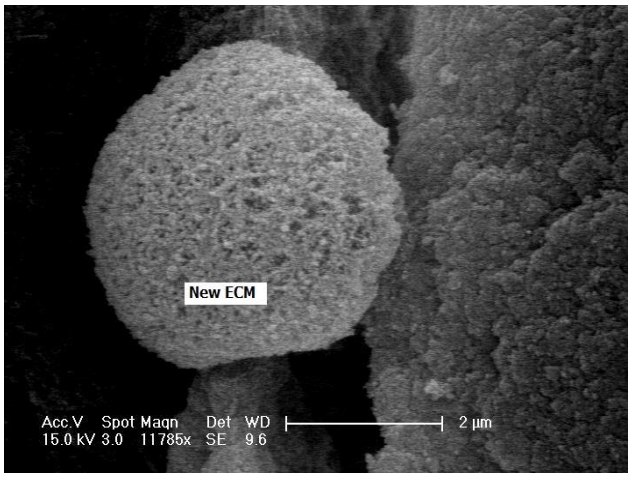

Figure 9 Material regeneration during fibroblast cell tests